LiDAR Point Cloud Registration with Formal Guarantees

Matteo Marchi, Jonathan Bunton, Bahman Gharesifard, and Paulo Tabuada

Abstract— **In recent years, LiDAR sensors have become pervasive in the solutions to localization tasks for autonomous systems. One key step in using LiDAR data for localization is the alignment of two LiDAR scans taken from different poses, a process called scan-matching or point cloud registration. Most existing algorithms for this problem are heuristic in nature and local, meaning they may not produce accurate results under poor initialization. Moreover, existing methods give no guarantee on the quality of their output, which can be detrimental for safety-critical tasks. In this paper, we analyze a simple algorithm for point cloud registration, termed PASTA. This algorithm is global and does not rely on point-to-point correspondences, which are typically absent in LiDAR data. Moreover, and to the best of our knowledge, we offer the first point cloud registration algorithm with *provable error bounds*. Finally, we illustrate the proposed algorithm and error bounds in simulation on a simple trajectory tracking task.**

I. INTRODUCTION

LiDAR[1] sensing is quickly becoming commonplace in autonomous vehicles and robots. LiDAR sensors are accurate, inexpensive, and provide rich environment data, enabling a wealth of successful work in localization and Simultaneous Localization and Mapping (SLAM) [1], [2], [3], [4]. To use LiDAR data effectively, these works typically rely on a crucial sub-routine for solving the point cloud registration problem.

Point cloud registration, also referred to as scan-matching, asks for the appropriate transformation relating two measurements of the same environment to one another. Typically, this transformation is simply a rotation and translation, but some more general settings also consider scaling and warps as well [5]. This problem has a standard closed-form solution when the point clouds from each measurement are also equipped with point-to-point correspondences, or when the point clouds are uniformly spaced with no noise [6]. In LiDAR sensor data, however, the associated point clouds have very non-uniform spacing and rarely contain perfect correspondences between points.

Despite these difficulties, a number of successful heuristic algorithms for point cloud registration have been developed. One of the simplest is the Iterative Closest Point (ICP) procedure [7], which tries to repeatedly establish valid correspondences and compute the associated transformations, seeking to minimize the incurred error in alignment. Numerous more exotic approaches exist with similar structure and intuition, such as the Normal Distributions Transform (NDT) [8] and various feature-based methods [4]. However, these methods usually require a good initial estimate of the transformation, or they rely on the existence of point-to-point correspondences that are absent in LiDAR data.

These existing algorithms for point cloud registration have shown good empirical performance in a variety of scenarios. They all, however, lack any formal guarantees on the quality of their proposed transformation. This type of error guarantee is *crucial* in safety-critical applications such as LiDAR-based localization for self-driving vehicles [9]. To the authors' knowledge, only one registration algorithm, TEASER++, provides such results in the form of a certification guarantee on the optimality of the computed transformation [5], which does not directly translate into an error guarantee. TEASER++, however, still relies on the existence of corresponding points in the LiDAR data.

In this paper, we show that a new algorithm recently proposed by the authors, Provably Accurate Simple Transformation Alignment (PASTA), which has precisely these missing guarantees. Moreover, it operates without requiring the existence of point correspondences, making it ideal for low-density LiDAR data. In our analysis of PASTA, we prove that its simple, globally valid algorithm has an explicit bound on the error between its output and the true transformation relating two point clouds. As already pointed out, these bounds may be instrumental, for example, in guaranteeing the safety of autonomous systems, but also in defining a supervisor for other heuristic and learning-based methods.

II. PRELIMINARIES

We begin by introducing some notation and concepts. The results we prove hold in $\mathbb{R}^n$ for any $n \in \mathbb{N}$, but when dealing with point clouds coming from LiDAR data, n will be 2 or 3.

1) A point cloud is a finite set with $d \in \mathbb{N}$ elements:
$$X = \{x^{(1)}, x^{(2)}, \dots, x^{(d)}\}, \tag{1}$$
where $x^{(i)} \in \mathbb{R}^n$ for each $i \in \{1, 2, \dots, d\}$.
2) Given a point cloud X, its convex hull is given by:
$$H = \left\{ x = \sum_{i=1}^{m} \lambda_i x^{(i)} \;\middle|\; \sum_{i=1}^{m} \lambda_i = 1, \lambda_i \geq 0 \right\}. \tag{2}$$
3) Given a compact set $H \subset \mathbb{R}^n$, and the Lebesgue measure μ on $\mathbb{R}^n$, we denote the volume of H as:
$$|H| = \mu(H) = \int_H \mathrm{d}\mu, \tag{3}$$

This research was supported in part by US ARL Cooperative Agreement W911NF-17-2-0196, NSF 2211146, and NSF 1705135.

M. Marchi, J. Bunton, B. Gharesifard, and P. Tabuada are with the Electrical and Computer Engineering Department, University of California at Los Angeles, Los Angeles, CA 90095 USA. {matmarchi, j.bunton, gharesifard, tabuada}@ucla.edu

[1]Light Detection and Ranging.

and define its radius as:

$$\rho(H) = \min_{q\in\mathbb{R}^n} \max_{x\in H} \|x - q\|. \tag{4}$$

4) We define the first moment of a compact set $H \subset \mathbb{R}^n$ as:

$$c = |H|^{-1} \int_{x\in E} x \, \mathrm{d}\mu. \tag{5}$$

5) We define the second moment of a compact set $H \subset \mathbb{R}^n$ relative to its first moment c as:

$$\Sigma = |H|^{-1} \int_{x\in H} (x - c)(x - c)^T \, \mathrm{d}\mu. \tag{6}$$

6) Given an orthornormal matrix $R \in \mathcal{SO}(n)$ and a set $H \subset \mathbb{R}^n$, we denote the rotated set as $RH \subset \mathbb{R}^n$:

$$RH = \{z \in \mathbb{R}^n \mid z = Rx, \ x \in H\}. \tag{7}$$

7) Given two compact sets $H_1, H_2 \subset \mathbb{R}^n$ of non-zero measure, we introduce a notion of "overlap" between them. This overlap is represented by a number $\delta \in [0, 1]$, and is defined as follows:

$$\delta = \frac{|H_1 \cap H_2|}{\max\{|H_1|, |H_2|\}}. \tag{8}$$

Intuitively, when $\delta = 0$, H_1 and H_2 are disjoint, and when $\delta = 1$, $H_1 = H_2$.

8) Integral expressions without a specified domain are interpreted as over all of $\mathbb{R}^n$.

III. Problem Statement

In [10] we presented PASTA: a methodology for computing the rigid transformation between point clouds generated from LiDAR data taken at different positions in the same environment, and empirically evaluated its effectiveness. Our aim in this paper is to provide deterministic bounds on the error in the translation $\hat{p}$ and rotation $\hat{R}$ computed by PASTA when the point clouds are not exactly related by a rigid transformation. This phenomenon occurs in practice because of sensor noise and finite LiDAR resolution (see Fig. 1).

Explicitly, we are given two point clouds X_1, X_2' corresponding to measurements taken at two distinct poses, related by the transformation (p, R). We use the notation X_2' here to emphasize that X_1 and X_2 are *not* related by a simple rotation and translation. We then compute the convex hulls of both point clouds, denoted by H_1 and H_2', and provide these as input to PASTA in (15). In the following sections, we derive worst case bounds on the errors $\|\hat{R} - R\|$ and $\|\hat{p} - p\|$, where $(\hat{p}, \hat{R}) = \text{PASTA}(H_1, H_2')$.

We conclude by presenting simulation results for PASTA and its error bounds in a closed-loop control task.

IV. Approach

In this section we provide a mathematical description of PASTA. Readers interested in its implementation and empirical evaluation are referred to [10]. The first observation is that PASTA directly operates on infinite sets rather than finite point clouds. We compute these infinite sets by first computing the convex hulls of the point clouds. There are advantages associated to this choice, particularly when dealing with LiDAR data, that are explored in [10].

A. Ideal Case

PASTA is most easily understood for two compact sets $H_1, H_2 \subset \mathbb{R}^n$ that are perfectly related by a rigid transformation $H_2 = RH_1 + p$. Under this relationship, the first and second moments of H_1 and H_2 are related by the expressions:

$$\begin{aligned} c_2 &= Rc_1 + p \\ \Sigma_2 &= R\Sigma_1 R^T. \end{aligned} \tag{9}$$

These equations can easily be obtained by directly computing c_2 and Σ_2, using the change of variables $x = Rz + p$:

$$\begin{aligned} c_2 = \frac{\int_{H_2} x \, \mathrm{d}\mu}{\int_{H_2} \mathrm{d}\mu} &= \frac{\int_{H_1} (p + Rz)\det(R) \, \mathrm{d}\mu}{\int_{H_1} \det(R) \, \mathrm{d}\mu} \\ &= p + R|H_1|^{-1} \int_{H_1} z \, \mathrm{d}\mu \\ &= p + Rc_1, \end{aligned} \tag{10}$$

noting that $\det(R) = 1$ by the orthonormality of R. Similarly:

$$\begin{aligned} \Sigma_2 &= \frac{\int_{H_2} (x - c_2)(x - c_2)^T \, \mathrm{d}\mu}{\int_{H_2} \mathrm{d}\mu} \\ &= \frac{\int_{H_2} (x - (p + Rc_1))(x - (p + Rc_1))^T \, \mathrm{d}\mu}{\int_{H_2} \mathrm{d}\mu}. \end{aligned} \tag{11}$$

Using the change of variables $x = p + Rz$, we obtain that:

$$\begin{aligned} \Sigma_2 &= \frac{\int_{H_1} R(z - c_1)(z - c_1)^T R^T \, \mathrm{d}\mu}{\int_{H_1} \mathrm{d}\mu} \\ &= R\Sigma_1 R^T. \end{aligned} \tag{12}$$

PASTA's estimate is then defined as the solution of (9) in terms of (p, R). In particular, the solution is given by

$$\begin{aligned} R &= V_2 V_1^T \\ p &= c_2 - Rc_1, \end{aligned} \tag{13}$$

where $V_1, V_2 \in \mathbb{R}^{n\times n}$ are the matrices whose columns are the unit-eigenvectors of Σ_1, Σ_2 respectively. We can verify this solution by directly substituting, noting that because R is orthogonal, (9) implies that Σ_1 and Σ_2 have the same eigenvalues, and thus their eigenvalue decompositions are:

$$\begin{aligned} \Sigma_1 &= V_1\Lambda_1 V_1^T = V_1 \Lambda V_1^T \\ \Sigma_2 &= V_1\Lambda_2 V_1^T = V_2 \Lambda V_2^T, \end{aligned} \tag{14}$$

where $\Lambda \in \mathbb{R}^{n\times n}$ is the diagonal matrix containing the eigenvalues of Σ_1 and Σ_2. It is then straightforward to verify that (9) is satisfied by the solution (13).

Before proceeding further, we clarify some technical details regarding the solution (13). First, there is a sign ambiguity on R, as both $V_2V_1^T$ and $-V_2V_1^T$ are valid solutions of (9). This ambiguity is generally resolved by using additional information about the sets H_1 and H_2, such as the various examples provided in [10]. Second, in order for $\Lambda_1 = \Lambda_2 = \Lambda$ to hold in (14), we need to fix an ordering for the eigenvalues of the second moments. To define this ordering, we require the eigenvalues of Σ_1 and Σ_2 to be simple. These eigenvalues characterize the magnitude of variations along the principal axes of H_1 and H_2, so this assumption essentially requires the environment to be sufficiently *asymmetric*.

With these considerations, given two compact sets H_1 and H_2, we define the output of PASTA as:

$$(\hat{p}, \hat{R}) = \text{PASTA}(H_1, H_2) = \left(c_2 - V_2 V_1^T c_1, V_2 V_1^T\right). \quad (15)$$

B. Non-Ideal Case

As shown above, PASTA's output is exact when the sets H_1, H_2 are exactly related by a rigid transformation. We now explore what happens when trying to reconstruct (p, R) using (15) when this is no longer the case.

In practice, the sets H_1 and H_2 are constructed by computing the convex hulls of point clouds corresponding to LiDAR scans of some shape or environment. These scans typically do not sample the same points and are affected by noise, as shown in Fig. 1. Consequently, the relationship $H_2 = RH_1 + p$ will not hold. Instead we will have $H_2' = RH_1' + p$, where H_2' is the rigid transformation of the "perturbed" convex hull H_1', with the perturbation caused by the difference in sampled points and noise.

Given the convex hulls H_1, H_1', and H_2', we consider their respective second moments Σ_1, Σ_1', and Σ_2', with eigenvalue decompositions defined by:

$$\Sigma_1 = V_1 \Lambda_1 V_1^T, \quad \Sigma_1' = V_1' \Lambda' V_1'^T, \quad \Sigma_2' = V_2' \Lambda' V_2'.$$

Applying (15) to the sets H_1 and H_2', i.e. $(\hat{p}, \hat{R}) = \text{PASTA}(H_1, H_2')$, the estimated rotation $\hat{R}$ is:

$$\hat{R} = V_2' V_1^T. \quad (16)$$

Note that the following relationship holds:

$$\begin{aligned} \Sigma_2' &= R \Sigma_1' R^T \\ V_2' \Lambda' V_2'^T &= R V_1' \Lambda' V_1'^T R^T, \end{aligned} \quad (17)$$

implying that $V_2' = RV_1'$ and $\hat{R} = RV_1' V_1^T$.

If we define $V_1' = EV_1$ for some error rotation matrix $E \in \mathcal{SO}(n)$ (which always exists since $V_1, V_1' \in \mathcal{SO}(n)$) , we arrive at

$$\hat{R} = REV_1 V_1^T = RE. \quad (18)$$

Consequently, since R preserves the Frobenius norm, we can write the distance between $\hat{R}$ and the real rotation R as:

$$\|\hat{R} - R\| = \|RE - R\| = \|R(E - I)\| = \|E - I\|, \quad (19)$$

which captures how close the error rotation E is to the identity (the null rotation).

Similarly, under these non-ideal conditions, the translation vector estimated by PASTA is:

$$\hat{p} = c_2' - \hat{R} c_1, \quad (20)$$

and if we define $e = c_1' - c_1$ as the difference in the first moments of H_1' and H_1, we can bound the difference between the estimated and the real translation vector as:

$$\begin{aligned} \|\hat{p} - p\| &= \|c_2' - \hat{R} c_1 - c_2 + R c_1\| \\ &= \|p + Rc_1' - REc_1 - p - Rc_1 + Rc_1\| \\ &= \|R(c_1 + e) - REc_1\| \\ &= \|R((I - E)c_1 + e)\| \\ &= \|(I - E)c_1 + e\| \le \|I - E\| \|c_1\| + \|e\|, \end{aligned} \quad (21)$$

where the first equality holds due to the relationships $H_2 = RH_1 + p$ and $H_2' = RH_1' + p$, and the final equation holds because R is norm preserving.

In section V, we provide bounds on $\|e\| = \|c_1' - c_1\|$ and $\|I - E\| = \|I - V_1' V_1^T\|$, parameterized by how "close" H_1' is to H_1 in a manner described next. Note again that the "closeness" of H_1' and H_1 is determined by the measurement noise and non-uniform sampling effects in the LiDAR sensor.

C. Perturbation Measure

The bounds that we will provide shortly are expressed as functions of the size of H_1 and H_1', described by $\rho(H_1 \cup H_1')$, and an overlap parameter δ defined in (8) that describes how close H_1 is to H_1'. Fig. 1 illustrates how point clouds generated from LiDAR measurements in different positions of a rectangular room sample different points, resulting in these different and non-overlapping convex hulls. Moreover, as the LiDAR resolution increases and its measurement noise lowers, there is greater overlap between H_1 and H_1'.

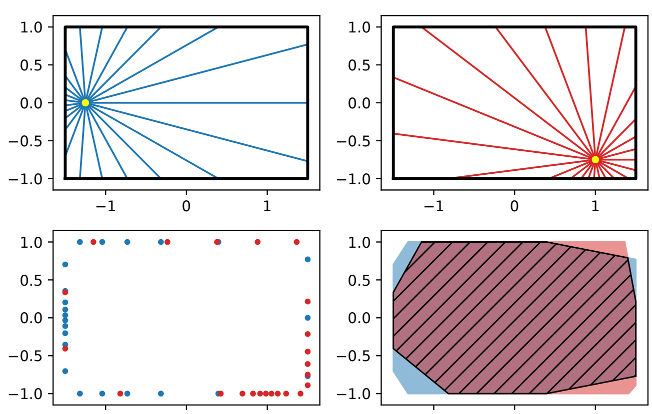

Fig. 1. Top row: LiDAR rays from different positions in a 2D environment. Bottom left: point clouds corresponding to the two measurements (blue is the first measurement, red is the second). Bottom right: hulls of the two point clouds and their intersection (hatched region). Here, δ is the surface area of the hatched region divided by the greatest of the areas of the two hulls.

V. THEORETICAL RESULTS

We now present the main results. First, we describe a bound on the difference of the first moments of two compact sets $H, H' \subset \mathbb{R}^n$ depending on their overlap δ and their size, expressed as the radius of $H \cup H'$.

Theorem 1 (**First moment perturbation**): Let $H, H' \subset \mathbb{R}^n$ be compact sets of non-zero measure, and let their first moments be $c, c' \in \mathbb{R}^n$ respectively. Further, let the overlap between H and H' be $\delta \in [0,1]$. Then:

$$\|c' - c\| \leq 2(1-\delta)\rho(H \cup H'). \tag{22}$$

Proof: First, let the vector $b \in \mathbb{R}^n$ be such that:

$$b \in \operatorname*{argmin}_{b \in \mathbb{R}^n} \max_{x \in H \cup H'} \|x - b\|, \tag{23}$$

which exists by compactness of $H \cup H'$. Then, we write:

$$\begin{aligned} \|c' - c\| &= \|c' - b - (c - b)\| \\ &= \left\| \frac{1}{|H'|} \int_{x \in H'} (x - b)\, \mathrm{d}\mu - \frac{1}{|H|} \int_{x \in H} (x - b)\, \mathrm{d}\mu \right\|. \end{aligned} \tag{24}$$

Before computing the bound, we observe that the first moment of a compact set is the expected value of a uniform probability distribution with that set as a support. To simplify the following expressions we define the indicator function:

$$\mathbf{1}_H(x) = \begin{cases} 1, & x \in H \\ 0, & \text{else.} \end{cases} \tag{25}$$

Then, we can write the uniform distribution over H' evaluated at any point $x \in \mathbb{R}^n$ as:

$$\begin{aligned} \frac{\mathbf{1}_{H'}(x)}{|H'|} &= \frac{\mathbf{1}_{H'}(x)}{|H'|} + \frac{\mathbf{1}_{H}(x)}{|H|} - \frac{\mathbf{1}_{H}(x)}{|H|} \\ &\quad + \frac{\mathbf{1}_{H \cap H'}(x)}{\max\{|H|, |H'|\}} - \frac{\mathbf{1}_{H \cap H'}(x)}{\max\{|H|, |H'|\}} \\ &= \frac{\mathbf{1}_{H}(x)}{|H|} + f_+(x) - f_-(x), \end{aligned} \tag{26}$$

where we have defined f_+ and f_- as:

$$\begin{aligned} f_+(x) &= \frac{\mathbf{1}_{H'}(x)}{|H'|} - \frac{\mathbf{1}_{H \cap H'}(x)}{\max\{|H|, |H'|\}} \\ f_-(x) &= \frac{\mathbf{1}_{H}(x)}{|H|} - \frac{\mathbf{1}_{H \cap H'}(x)}{\max\{|H|, |H'|\}}. \end{aligned}$$

Observe that f_+ and f_- are non-negative, and by definition of δ enjoy the following property:

$$\int f_+(x)\, \mathrm{d}\mu = \int f_-(x)\, \mathrm{d}\mu \leq 1 - \delta. \tag{27}$$

We can now directly compute:

$$\begin{aligned} \|c' - c\| &= \left\| \int (x - b) \frac{\mathbf{1}_{H'}}{|H'|}\, \mathrm{d}\mu - \int (x - b) \frac{\mathbf{1}_{H}}{|H|}\, \mathrm{d}\mu \right\| \\ &= \left\| \int (x - b)\,(f_+ - f_-)\, \mathrm{d}\mu \right\| \\ &\leq \int \|x - b\|\,(|f_+| + |f_-|)\, \mathrm{d}\mu \\ &\leq 2(1-\delta)\rho(H \cup H'). \end{aligned} \tag{28}$$

■

We now prove an analogous result bounding the difference between the second moments of two compact sets H and H' in terms of their overlap, δ.

*Theorem 2 (***Second moment perturbation***):* Let $H, H' \subset \mathbb{R}^n$ be compact sets of non-zero measure, and let their second moments be $\Sigma, \Sigma' \in \mathbb{R}^{n \times n}$ respectively. If the overlap between H and H' is some $\delta \in [0,1]$, then:

$$\|\Sigma' - \Sigma\| \leq \left(2(1-\delta) + 4(1-\delta)^2\right) \rho^2(H \cup H'). \tag{29}$$

Proof: Identically to the proof of Theorem 1, the second moments of H and H' can be expressed as the second moments of uniform distributions whose supports are H and H' respectively. Then, defining $\Delta c = c' - c$ we write:

$$\begin{aligned} \|\Sigma' - \Sigma\| &= \Bigg\| \int (x - c')(x - c')^T \frac{\mathbf{1}_{H'}}{|H'|}\, \mathrm{d}\mu \\ &\qquad - \int (x - c)(x - c)^T \frac{\mathbf{1}_{H}}{|H|}\, \mathrm{d}\mu \Bigg\| \\ &= \Bigg\| \int (x - c')(x - c')^T\,(f_+ - f_-)\, \mathrm{d}\mu \\ &\quad - \int \left(\Delta c \Delta c^T - (x - c)\Delta c^T - \Delta c (x - c)^T\right) \frac{\mathbf{1}_{H'}}{|H'|}\, \mathrm{d}\mu \Bigg\| \\ &= \Bigg\| \int (x - c')(x - c')^T\,(f_+ - f_-)\, \mathrm{d}\mu \\ &\quad - \left(\Delta c \Delta c^T - (c' - c)\Delta c^T - \Delta c (c' - c)^T\right) \Bigg\| \\ &\leq \left\| \int (x - c')(x - c')^T\,(f_+ - f_-)\, \mathrm{d}\mu \right\| + \left\|\Delta c \Delta c^T\right\| \\ &\leq \rho^2(H \cup H') \int (|f_+| + |f_-|)\, \mathrm{d}\mu + 4(1-\delta)^2 \rho^2(H \cup H') \\ &\leq \left(2(1-\delta) + 4(1-\delta)^2\right) \rho^2(H \cup H'), \end{aligned}$$

where the penultimate inequality is obtained by noting that $\|\Delta c\| \leq 2(1-\delta)\rho(H \cup H')$ by Theorem 1. ■

Following (13), PASTA uses the unit eigenvectors of the second moments to estimate the relative rotation between frames. We are therefore interested in bounding the change in these eigenvectors as a function of the perturbation of the second moment. We prove precisely this bound in the following result.

*Lemma 1 (***Eigenvector perturbation***):* Let $A, B \in \mathbb{R}^{n \times n}$ be symmetric matrices, with A positive definite. Suppose that all eigenvalues of A are simple, and $2\|B\| < \min_{i \neq j} |\lambda_i - \lambda_j|$, $i, j \in \{1, 2, \ldots, n\}$, with λ_i denoting the i-th eigenvalue of A. Then:

$$\|u_i' - u_i\| \leq -\frac{1}{2} \ln\left(1 - \frac{2\|B\|}{\min_{i \neq j} |\lambda_i - \lambda_j|}\right), \tag{30}$$

where u_i' and u_i are the i-th unit eigenvectors of A and $A + B$, respectively.

Proof: First, consider $A + tB$, with $t \in [0,1]$, and let $\lambda_i(t), u_i(t)$ be the i-th eigenvalue and unit-eigenvector of $A + tB$, respectively. From the perturbation analysis in [11, Chapter 2], we can bound the derivative of the eigenvalues of $A + tB$ with respect to t as:

$$\left| \frac{\partial \lambda_i}{\partial t}(t) \right| \leq \|B\|, \tag{31}$$

which implies that $|\lambda_i(t) - \lambda_i(0)| \leq t\|B\|$. Consequently:

$$\min_{i \neq j} |\lambda_i(t) - \lambda_j(t)| \geq \min_{i \neq j} |\lambda_i(0) - \lambda_j(0)| - 2\|B\| t. \tag{32}$$

This holds because each eigenvalue can change by at most $\|B\|$, and if the initial distance between any pair is greater than $2\|B\|$, the eigenvalues $\lambda_i(t)$ are simple for all $t \in [0,1]$.

Using [12, Corollary 4], we also know that:

$$\begin{aligned} \left\| \frac{\partial u_i}{\partial t}(t) \right\| &\leq \frac{\|B\|}{\min_{i\neq j} |\lambda_i(t) - \lambda_j(t)|} \\ &\leq \frac{\|B\|}{\min_{i\neq j} |\lambda_i - \lambda_j| - 2\|B\|t}, \end{aligned} \tag{33}$$

from which we establish:

$$\begin{aligned} \|u_i(1) - u_i(0)\| &\leq \int_0^1 \left\| \frac{\partial u_i}{\partial t}(t) \right\| \mathrm{d}t \\ &\leq \int_0^1 \frac{\|B\|}{\min_{i\neq j} |\lambda_i - \lambda_j| - 2\|B\|t} \\ &= -\frac{1}{2} \ln \left(1 - \frac{2\|B\|}{\min_{i\neq j} |\lambda_i - \lambda_j|} \right). \end{aligned} \tag{34}$$

■

Finally, we derive an additional result that relates the perturbation of the eigenvectors to the perturbation of the corresponding rotation matrices constructed by PASTA.

*Lemma 2 (***Rotation perturbation***):* Let $U, V \in \mathbb{R}^{n\times n}$ be orthonormal and $\varepsilon \in \mathbb{R}_{\geq 0}$. Assume that:

$$\|u_i - v_i\| \leq \varepsilon \quad \text{for all } i = 1, 2, ..., n, \tag{35}$$

where u_i and v_i are the i-th columns of U and V, respectively. Then, the orthonormal matrix $R = U^T V$ is such that:

$$\|R - I\| \leq \varepsilon\sqrt{n}. \tag{36}$$

Proof: By direct computation:

$$\begin{aligned} \|R - I\|^2 &= \|U(R - I)\|^2 = \|V - U\|^2 \leq \|V - U\|_F^2 \\ &= \sum_{i=1}^{n} \|v_i - u_i\|^2 \leq \sum_{i=1}^{n} \varepsilon^2 = \varepsilon^2 n. \end{aligned} \tag{37}$$

The first equality holds because the 2-norm is invariant to multiplication by an orthonormal matrix, and $\|\cdot\|_F$ denotes the Frobenius norm. ■

We are now in a position to state the main result, which relates the overlap between H_1 and H_1', $\delta \in [0, 1]$, to the error in the position and rotation estimated by PASTA.

*Theorem 3 (***PASTA error bound***):* Let $H_1, H_1' \subset \mathbb{R}^n$ be non-empty compact sets of non-zero measure with an overlap of $\delta \in [0, 1]$. Let c be the first moment of H_1, and define:

$$e_c = 2(1-\delta)\rho(H_1 \cup H_1'), \text{ and}$$

$$e_\Sigma = \left(2(1-\delta) + 4(1-\delta)^2\right) \rho^2(H_1 \cup H_1').$$

Then, if $\min_{i,j} |\lambda_i - \lambda_j| > 2e_\Sigma$, where λ_i is the ith eigenvalue of the second moment of H_1, the following holds:

$$\begin{aligned} \|\hat{R} - R\| &\leq -\tfrac{\sqrt{n}}{2} \ln \left(1 - \tfrac{2e_\Sigma}{\min_{i\neq j} |\lambda_i - \lambda_j|} \right) \\ \|\hat{p} - p\| &\leq -\|c\| \tfrac{\sqrt{n}}{2} \ln \left(1 - \tfrac{2e_\Sigma}{\min_{i\neq j} |\lambda_i - \lambda_j|} \right) + e_c. \end{aligned} \tag{38}$$

Proof: By Theorems 1 and 2, we know that

$$\|c_1' - c_1\| \leq e_c \text{ and } \|\Sigma_1' - \Sigma_1\| \leq e_\Sigma.$$

Accordingly, we can write the perturbed second moment as $\Sigma_1' = \Sigma_1 + \Sigma_e$, with $\|\Sigma_e\| \leq e_\Sigma$. Applying Lemma 1 with $A = \Sigma_1$ and $B = \Sigma_e$, we have that:

$$\|u_i' - u_i\| \leq -\frac{1}{2} \ln \left(1 - \frac{2e_\Sigma}{\min_{i\neq j} |\lambda_i - \lambda_j|} \right), \tag{39}$$

with u_i' the ith eigenvector of Σ_1', u_i the ith eigenvector of Σ_1, and λ_i the ith eigenvalue of Σ_1. Finally, by applying Lemma 2 with $\varepsilon = -\frac{1}{2} \ln \left(1 - \frac{2e_\Sigma}{\min_{i\neq j} |\lambda_i - \lambda_j|} \right)$, we see:

$$\|\hat{R} - R\| = \|E - I\| \leq -\frac{\sqrt{n}}{2} \ln \left(1 - \frac{2e_\Sigma}{\min_{i\neq j} |\lambda_i - \lambda_j|} \right).$$

As for the translation, we can simply write the bound:

$$\begin{aligned} \|\hat{p} - p\| &\leq \|E - I\|\|c\| + \|c' - c\| \\ &\leq -\|c\| \frac{\sqrt{n}}{2} \ln \left(1 - \frac{2e_\Sigma}{\min_{i\neq j} |\lambda_i - \lambda_j|} \right) + e_c. \end{aligned}$$

■

The bounds in (38) depend on the size of the environment (described by ρ) and the achievable overlap (described by δ). While these bounds are always valid, it should be noted that in practice δ can be especially low in non-convex environments, because different parts of the environment are visible from different positions. Note that there is an additional dependence on the minimum separation in the eigenvalues of Σ. This quantity depends on how "asymmetric" the environment is. For example, a very long but thin room would have a high minimum separation.

Some additional remarks are in order. We note that explicitly computing the bounds requires knowledge of the parameter δ. One open question is if one can obtain a bound on the errors which only depends on knowledge of the size and shape of the environment, resolution of the LiDAR, and bounds on the measurement noise. In practice, an estimate for δ can easily be obtained via a calibration-like experiment, where the LiDAR sensor is used to collect point cloud data from multiple positions, and the overlaps of their hulls are evaluated. Empirically, we observe that the lowest overlaps – and therefore worst associated guarantees – occur at poses where the sensor is close to walls and corners.

VI. SIMULATION RESULTS

In this section, we illustrate the effectiveness of PASTA as a localization method in a simple simulated closed-loop trajectory tracking task[2]. Together with the simulation results, we show a numerical evaluation of the pose estimate bounds according to the theoretical analysis above.

Our simulation consists of a simple robot moving within a convex 2D environment that extends approximately 6m horizontally and 3m vertically. The robot possesses three degrees of freedom (horizontal position, vertical position, and angle) and obeys simple double integrator dynamics in each state,where $u_x, u_y, u_\omega \in \mathbb{R}$ are positional and angular acceleration control inputs. The system does not have access to the state, but instead receives a point cloud constructed from LiDAR measurements at the current pose.

In the experiment, the LiDAR data is produced with a resolution of $1°$ (360 rays), and the distance measurements are affected by zero mean Gaussian noise with a standard

[2]Results using a real LiDAR sensor in a non-control task can be found in [10]. Empirically we observed an average position estimation error below 10cm, and average angle estimation error below $1°$ in a room of size approximately 6m×3m. We also noted some inherent robustness to non-convexity in the environment.

deviation of 1cm. The values are picked to be comparable to the performance of available real-world LiDAR sensors.

The system is simulated using zero-order hold control inputs generated at a frequency of 100Hz. The controller consists of a simple full state feedback linear controller acting on a state estimate provided by a Luenberger observer. The Luenberger observer operates using only the pose estimate generated by PASTA from the LiDAR data.

We then ask the system to track a sinusoidal trajectory within the environment. A visualization of the environment and the trajectories is shown in Fig. 2.

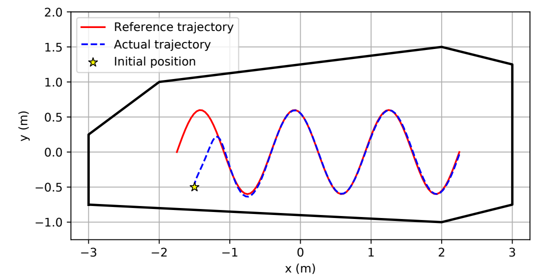

Fig. 2. Visualization of the environment, the reference and actual position trajectories in the closed-loop simulation.

We initialized the state of the system at a position within 0.75m and $45°$ of the reference trajectory with zero velocity. Similarly, the initial state estimate is chosen within 0.25m and $15°$ from the real initial state.

In Fig. 3, we show the error in state estimation when the Luenberger observer uses the pose estimate provided by PASTA as opposed to the true pose of the system. Notably, the errors are almost identical, with steady state errors in the order of centimeters and fractions of a degree.

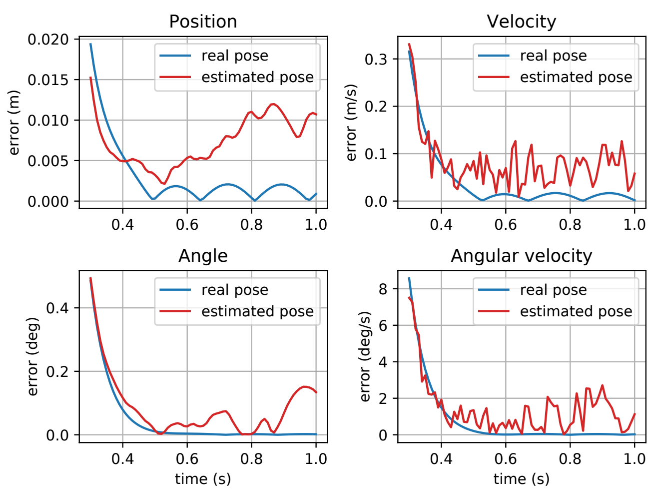

Fig. 3. Norm of the trajectory tracking error over time for the closed-loop control task with the observer fed by the real pose and the pose estimated by PASTA. We do not plot the initial transient for ease of visual comparison.

We also evaluate the numerical bounds for the pose estimate provided by PASTA along the trajectory, together with its actual incurred error, plotted using different scales, in Fig. 4. Note that the error bound on the norm of the rotation matrix is converted to a bound on the corresponding rotation angle for ease of interpretation. As expected, the worst case bound is conservative, with the actual error being at least an order of magnitude lower.

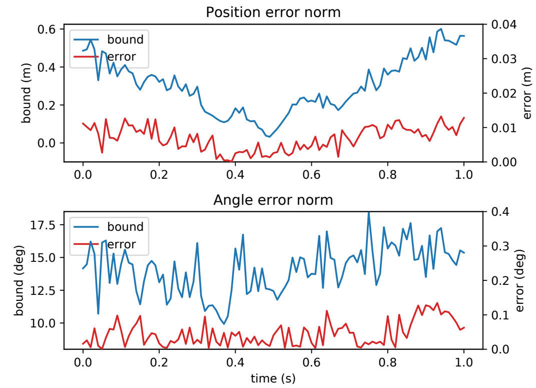

Fig. 4. Norms of the actual error of the pose estimated by PASTA along the trajectory compared with the error bound guaranteed by Theorem 3. Note the bound scale (left-hand side) differs from the actual error scale (right-hand side).

VII. CONCLUSIONS

In this paper, we analyzed a new algorithm for the point registration problem, termed PASTA. Our analysis produced hard error bounds for the estimated rigid transformation even when data is affected by noise and other non-idealities. We then demonstrated the effectiveness of our method and derived bounds in a simulated closed-loop control task. Given PASTA's theoretical guarantees, future work consists in extending PASTA to heavily non-convex environments and integrating it into a simple SLAM framework.

REFERENCES

[1] W. Hess, D. Kohler, H. Rapp, and D. Andor, "Real-time loop closure in 2D LIDAR SLAM," in *2016 IEEE International Conference on Robotics and Automation (ICRA)*. IEEE, 2016, pp. 1271–1278.

[2] C. Cadena, L. Carlone, H. Carrillo, Y. Latif, D. Scaramuzza, J. Neira, I. Reid, and J. Leonard, "Past, present, and future of simultaneous localization and mapping: Towards the robust-perception age," *IEEE Transactions on Robotics*, vol. 32, no. 6, p. 1309–1332, 2016.

[3] C. Debeunne and D. Vivet, "A review of visual-LiDAR fusion based simultaneous localization and mapping," *Sensors*, vol. 20, no. 7, p. 2068, 2020.

[4] L. Cheng, S. Chen, X. Liu, H. Xu, Y. Wu, M. Li, and Y. Chen, "Registration of Laser scanning point clouds: A review," *Sensors*, vol. 18, no. 5, p. 1641, 2018.

[5] H. Yang, J. Shi, and L. Carlone, "Teaser: Fast and certifiable point cloud registration," *IEEE Transactions on Robotics*, vol. 37, no. 2, pp. 314–333, 2020.

[6] B. Horn, "Closed-form solution of absolute orientation using unit quaternions," *Journal of the Optical Society of America*, vol. 4, no. 4, pp. 629–642, 1987.

[7] P. Besl and N. McKay, "Method for registration of 3-D shapes," in *Sensor fusion IV: control paradigms and data structures*, vol. 1611. Spie, 1992, pp. 586–606.

[8] P. Biber and W. Straßer, "The normal distributions transform: A new approach to Laser scan matching," in *Proceedings 2003 IEEE/RSJ International Conference on Intelligent Robots and Systems*, vol. 3. IEEE, 2003, pp. 2743–2748.

[9] R. Wolcott and R. Eustice, "Visual localization within LiDAR maps for automated urban driving," in *2014 IEEE/RSJ International Conference on Intelligent Robots and Systems*. IEEE, 2014, pp. 176–183.

[10] M. Marchi, J. Bunton, B. Gharesifard, and P. Tabuada. (2022, Mar) PASTA: Provably accurate simple transformation alignment. UCLA. [Online]. Available: https://gharesifard.github.io/pdfs/PASTA.pdf

[11] J. Wilkinson, *The algebraic eigenvalue problem*. Oxford University Press, Inc., 1988.

[12] C. Meyer and G. Stewart, "Derivatives and perturbations of eigenvectors," *SIAM Journal on Numerical Analysis*, vol. 25, no. 3, pp. 679–691, 1988.